

1

2 **The contribution of lincRNAs at the interface between cell cycle regulation**
3 **and cell state maintenance**

4 Adriano Biasini^{1,*}, Adam Alexander Thil Smith^{1,2,*}, Baroj Abdulkarim ¹, Jennifer Yihong Tan¹,
5 Maria Ferreira da Silva¹ and Ana Claudia Marques¹

6

7 ¹Department of Computational Biology, University of Lausanne, Switzerland

8 ² Current Address: Baker Heart & Diabetes Institute, 75 Commercial Road, Melbourne, Victoria
9 3004, Australia

10 *These authors contributed equally to the work

11

12

1 **ABSTRACT**

2 Cell cycle progression requires dynamic and tightly-regulated transitions between well-defined
3 cell cycle stages. These transitions are controlled by the interplay of established cell cycle
4 regulators. Changes in the activity of these regulators are thought to underpin differences in cell
5 cycle kinetics between distinct cell types. Here, we investigate whether cell type-specific long
6 intergenic noncoding RNAs (lincRNAs) contribute to embryonic stem cell adaptations, which have
7 been shown to be essential for the maintenance of embryonic stem cell state.

8 We used single cell RNA-sequencing data of mouse embryonic stem cells (mESC) staged as G1,
9 S, or G2/M to identify genes differentially expressed between these phases. We found
10 differentially expressed lincRNAs to be enriched amongst cell cycle regulated genes. These cell
11 cycle associated lincRNAs (CC-lincRNAs) are co-expressed with protein-coding genes with
12 established roles in cell cycle progression. Interestingly, 70% of CC-lincRNAs are differentially
13 expressed between G1 and S, suggesting they may contribute to the maintenance of the short
14 G1 phase that characterizes the embryonic stem cell cycle. Consistent with this hypothesis, the
15 promoters of CC-lincRNAs are enriched in pluripotency transcription factor binding sites, and their
16 transcripts are frequently co-regulated with genes involved in the maintenance of pluripotency.
17 We tested the impact of 2 CC-lincRNA candidates and show that modulation of their expression
18 is associated with impaired cell cycle progression, further underlining the contribution of mESC-
19 specific lincRNAs to cell cycle modulation in these cells.

20

21

1 INTRODUCTION

2 The cell cycle is a dynamic sequence of events leading from one parent cell to two daughter cells.
3 This requires replication of chromosomes during the Synthesis phase (S phase) and their
4 segregation into two daughter cells during Mitosis (M phase). M and S phases are separated by
5 2 Gap phases, G1 and G2, that act as checkpoints to prevent cell division without genome
6 replication and aberrant polyploidy [1]. Progression through cell cycle is regulated by cell cycle
7 stage-specific activation and repression of numerous proteins including Cyclin Dependent
8 Kinases (CDKs) and proteins from the Cyclin family [2]. In most somatic cells, the oscillatory
9 expression or activity of distinct Cyclin-Cdk complexes allows the activation and repression of cell
10 cycle regulators and promotes cell-cycle transitions [2]. One key regulator of this process is the
11 retinoblastoma protein (RB) that controls G1 and prevents entry into S phase. Upon entrance in
12 G1, RB is unphosphorylated (active) and blocks the expression of genes required for G1/S
13 transition. During G1, RB is phosphorylated and becomes inactive, allowing cells to progress to
14 S phase [3]. In embryonic stem cells (ESCs), RB is hyperphosphorylated, resulting in suppression
15 of the G1-S checkpoint and thereby rapid shuttling between DNA synthesis and mitosis,
16 decreasing the average duration of the ESC cell cycle [reviewed in [4]].

17 These significant adaptations in the ESC cell cycle are important for the maintenance of the
18 embryonic stem cell state and cell fate decisions, as highlighted by the partial overlap between
19 the gene regulatory networks that control the two processes [5]. For example, both Oct4 and
20 Nanog, two core pluripotency factors, control genes involved in cell cycle regulation: in mouse
21 ESCs (mESCs), Oct4 represses the expression of *p21*, a Cyclin-dependent kinase inhibitor that
22 is expressed in somatic cells but not in embryonic stem cells [6]; *NANOG*, whose expression is
23 cell cycle-regulated, controls S-phase entry by regulating the expression of *Cdc25C* and *CDK6* in
24 human ESCs (hESCs) [7]. While the association between cell cycle dynamics and cell state is
25 well established, the molecular mechanisms underlying this connection remain uncharacterized
26 [5].

27 In addition to proteins, noncoding RNAs, including long intergenic noncoding RNAs (lincRNAs),
28 have also been shown to contribute to cell cycle progression [8]. An example of this is MALAT1,
29 a lincRNA that is frequently upregulated in multiple human cancers [9]. In human fibroblasts,
30 depletion of MALAT1 leads to decreased expression of several genes involved in cell cycle
31 progression and results in G1 arrest. MALAT1 is also involved in splicing of *B-Myb*, a gene
32 involved in the transcriptional regulation of several mitotic proteins [10]. More recently, the
33 cohesion regulator long noncoding RNA (CONCR) has been found to be necessary for cell cycle

1 progression and DNA replication. CONCR expression is activated by the transcription factor MYC
2 and is upregulated in multiple cancer types [11]. Silencing of CONCR leads to a significant
3 decrease in DNA synthesis. At the molecular level, CONCR physically interacts with DDEA/H-
4 boy helicase 11, which ensures the proper separation of sister chromatids during the cell division
5 process. The absence of CONCR leads to the loss of sister chromatid cohesion and affects
6 metaphase [11]. Finally, lincRNA expression is often dysregulated in cancer and the
7 characterization of subsets of cancer-associated lincRNAs highlights their potential roles as cell
8 cycle progression modulators [12, 13].

9 LincRNAs are also part of the network controlling stem cell fate maintenance and differentiation
10 [14]. Because lincRNA expression is often tissue-specific [15, 16], in contrast to proteins, we
11 hypothesized they can support cell type-specific activity of ubiquitously-expressed genes and act
12 at the intersection of cell cycle and mESC cell state regulation. The ability of tissues specific
13 noncoding RNAs to modulate the activity of ubiquitously expressed gene was already exemplified
14 by IncSCA7. This lincRNA regulates ATXN7 levels in retinal and cerebellar neurons and
15 contributes to specific degeneration of this cells in SCA7 patients [17]. Additionally, the relative
16 short half-lives of lincRNAs [18, 19] further underscores their potential as modulators of temporally
17 resolved processes such as cell cycle progression.

18 Here, we investigate the contributions of lincRNAs to embryonic stem cell cycle adaptations.

19

1

2 RESULTS

3 **LincRNA expression is often cell-cycle regulated.**

4 We used publicly-available single-cell RNA-sequencing (scRNAseq) data for 279 mouse
5 embryonic stem cells with known cell cycle stage [20] to assess the extent of cell cycle-regulated
6 lincRNA expression in mouse embryonic stem cells (mESCs). We estimated the expression of
7 protein-coding transcripts and lincRNAs in each of these cells. After excluding cells and genes
8 that failed quality control (Supplementary Figure 1) we identified 10 487 genes, including 781
9 lincRNAs, whose expression can be robustly detected in 246 cells. As previously shown [20],
10 gene expression patterns in this dataset reflect the cell cycle stages of the individual cells (Figure
11 1A), supporting its use to identify transcripts whose expression are cell-cycle dependent. Using
12 DEseq2, we identified 638 genes (6.1%) whose expression is significantly different between at
13 least 2 cell cycle stages (Supplementary table 1). The proportion of differentially expressed
14 lincRNAs (n=70, 8.96%) is significantly higher than found for protein-coding genes (n=501,
15 5.51%) (proportions test p-value < 0.05, Figure 1B, Supplementary Table 1), indicating that
16 lincRNA expression is more dynamic throughout the mESC cell cycle than is the expression of
17 protein-coding genes.

18 The median expression of mRNAs is roughly 14 times higher than that of lincRNAs
19 (Supplementary Figure 2A) and steady state abundance can impact the ability to detect
20 differential gene expression, as highlighted by the significantly higher expression (two-tailed
21 Wilcoxon test, p-value < 2×10^{-16}) of genes identified as differentially expressed (Supplementary
22 Figure 2A). To assess whether lincRNAs' relatively low expression impacts our differential gene
23 expression analysis results, we repeated the analysis by re-quantifying protein-coding gene
24 expression using a subset (1/14) of randomly sampled reads from each library. At this sequencing
25 depth, the median mRNA expression is comparable to that of lincRNAs in the full data
26 (Supplementary Figure 2B). We repeated expression quantification, quality control, normalization,
27 filtering and differential gene expression analyses using these randomly sampled reads and found
28 that only 60% of the mRNAs found to be differentially expressed using the full data are also
29 differentially expressed when using the down-sampled libraries. This result indicates that the
30 higher proportion of differentially expressed lincRNAs is likely an underestimate due to the limited
31 power to measure their expression using single cell RNA sequencing data.

32 To validate our *in silico* differential gene expression predictions we used DNA content to sort
33 mESC cells into G1, S and G2/M stages and measured the cell cycle stage expression of 12

1 differentially expressed lincRNAs, including *Neat1*, and 3 mESC cell cycle protein-coding genes
2 (*Ccnb1*, *Ccnd1* and *Ccne1*) by quantitative PCR (Figure 1C, Supplementary Figure 3). The cell
3 cycle protein coding gene and lincRNA expression patterns measured by qPCR were generally
4 consistent with what was estimated using scRNA sequencing data. The results of this analysis
5 support that despite the relatively low expression of lincRNAs that complicates the accurate
6 estimation of their expression, our differential expression predictions are generally robust.

7

8 **Differentially expressed lincRNAs contribute to the regulation of cell cycle progression.**

9 Consistent with the role of differentially expressed protein-coding genes in the regulation of cell
10 cycle progression, these genes are significantly enriched (hypergeometric test adjusted p-value
11 < 0.001) in annotations with gene ontology terms such as “cell division” and other related cell-
12 cycle processes (Figure 2A). Furthermore, 8.8% (44 of 501) of differentially expressed protein-
13 coding loci are orthologous to genes previously shown to have a periodic expression throughout
14 the human cell cycle [21], a significant 3.1-fold enrichment relative to all mESC expressed protein-
15 coding loci (214, hypergeometric test p-value < 0.05). These results support that genes
16 differentially expressed between cell cycle stages are indeed enriched in cell cycle regulators.

17 The enrichment of cell-cycle related genes amongst those differentially expressed between cell-
18 cycle stages suggests that some of the lincRNAs identified here as differentially expressed might
19 also contribute to mESC cell cycle regulation. Most lincRNAs differentially expressed between
20 cell cycle stages were annotated *de novo* (53 *de novo* lincRNAs) using mESC RNA sequencing
21 data [22]. We searched the literature for functions of the remaining 17 differentially expressed
22 lincRNAs annotated by ENSEMBL. Of these, only 4 have been previously characterized: *Neat1*,
23 *Malat1*, the host transcript for *snord93*, and *miRNA-24* pri-miRNA transcript. *Malat1* is a cancer-
24 associated lincRNA and has been previously implicated in cell cycle progression. For example,
25 *Malat1* is highly expressed during the S and M phases of human Fibroblasts where it controls cell
26 cycle-related processes [10]. *Neat1*, whose knockdown was recently shown to impair S phase
27 transition [23] has also been frequently associated with cancer and cell cycle progression [24].
28 Relatively little is known about *snord93* but changes in this RNA’s levels impact cell proliferation
29 [25], which would be consistent with a role in cell cycle progression. Finally, *miRNA-24* post-
30 transcriptionally regulates *MYC* and *E2F2*, two known cell cycle genes, and changes in its levels
31 impair G1 transition [26]. In conclusion, all of the 4 annotated and characterized lincRNAs we
32 identified as being differentially expressed either have established roles or have been associated
33 with cell cycle progression.

1 Given the paucity of functional annotations for lincRNAs, and to assess broadly the contributions
2 of differentially expressed lincRNAs to the cell cycle, we reasoned that genes that functionally
3 participate in cell cycle regulation should genetically interact with known cell cycle regulators. To
4 first validate this idea, we considered cell cycle phase differentially expressed protein-coding
5 genes not annotated as cell cycle regulators, and found their expression is more often significantly
6 ($p < 0.001$, Wilcoxon rank sum test) correlated with the expression of annotated cell-cycle genes
7 than non-differentially expressed protein-coding loci (Figure 2B). Similarly, we found that the
8 expression of differentially expressed lincRNAs is also significantly more often correlated with the
9 levels of cell cycle genes than non-differentially expressed lincRNAs (Figure 2C, $p < 0.001$
10 Wilcoxon rank sum test), supporting their contributions to mESC cell cycle progression. Hereafter,
11 we refer to differentially expressed lincRNAs and protein-coding genes as cell-cycle associated
12 lincRNAs and protein coding genes, or CC-lincRNAs and CC-PCGs, respectively.

13

14 **Cell cycle lincRNAs are associated with stem cell cycle adaptations**

15 The cell cycle is a ubiquitous process, yet most lincRNAs are expressed in cell-type specific
16 manner [27]. Do the CC-lincRNAs identified here contribute to cell cycle regulation ubiquitously,
17 or are their functions restricted to mESCs? To gain initial insights into this question we used
18 publicly available transcriptome-wide data [28] to estimate the tissue specificity of lincRNAs and
19 protein coding genes across 29 adult and developing mouse tissue and cell lines. We estimated
20 Tau, a measure of tissue specificity, for CC-lincRNAs, CC-PCGs and known cell cycle regulators.
21 Tau varies between 0% for “ubiquitously expressed” to 100% for “tissue-specifically expressed”
22 genes [29]. As expected, CC-PCGs, as well as established cell-cycle genes, are broadly
23 expressed (median tau=24.8%). In contrast, CC-lincRNAs are significantly more tissue specific
24 (median tau=42%, Wilcox rank sum test p -value < 0.05 , Figure 3A) than their protein-coding
25 counterparts, and are as tissue-specific as other mESC expressed lincRNAs (data not shown).

26 To further test if CC-lincRNA expression is often restricted to mESCs, we investigated changes
27 in their transcript abundance upon neuronal differentiation of mESCs. *In vitro* neural differentiation
28 is a well-defined and highly efficient process (>80% of differentiated cells). We took advantage of
29 publicly-available transcriptome-wide expression for a time-course of neuronal commitment of
30 mESC [30] to investigate the changes in noncoding and coding gene expression. Consistent with
31 their tissue-specific expression (Figure 3A), CC-lincRNA expression decreases rapidly upon
32 differentiation (Figure 3B), supporting their contribution to cell cycle regulation being restricted to

1 mESCs. In contrast, CC-PCGs are expressed at similar levels throughout neuronal commitment
2 (Figure 3C).

3 The transcriptional network controlling mESC cell state and function is regulated by a set of mESC
4 core transcription factors [31]. The short G1 phase that characterizes the embryonic stem cell
5 cycle, which is critical to ensure maintenance of pluripotency, is in part orchestrated by stem cell-
6 specific factors [32]. We took advantage of publicly available data ChIP-seq data for pluripotency
7 transcription factors in mESCs [33], to assess the extent of these factors' binding of to cell-cycle
8 regulated lincRNA promoters. We found that CC-lincRNA promoters are enriched in mESC core
9 transcription factors (TFs) supporting their role in the network underlying mESC cell state.
10 Specifically, promoters of CC-lincRNAs are significantly enriched, relative to all expressed
11 lincRNAs, in the binding of pluripotency transcription factors, including Nanog, Oct4 and Sox2
12 (FDR<0.05, permutation test) (Figure 3D). We found no significant enrichment by most
13 pluripotency TFs at the promoters of CC-PCGs (Figure 3D).

14 To assess what aspect of mESC cell cycle progression might be more often modulated by CC-
15 lincRNAs, we investigated their relative expression across different cell cycle phases. Consistent
16 with previous observations that mRNA expression peaks at G2/M phase in human cells [34, 35]
17 we found that CC-protein-coding genes were highly expressed in S and G2/M (Figure 3E) and
18 were often differentially expressed between G1 vs G2/M (Figure 3F). In contrast, the levels of
19 CC-lincRNAs were higher in G1 relative to all other cell cycle stages (Figure 3E) and most were
20 differentially expressed between G1 *versus* S phase (Figure 3F). In total, 70% of all CC-lincRNAs
21 are differentially expressed between G1 and another cell cycle stage.

22 Given the significantly elevated expression of CC-lincRNAs in G1, their tissue-specific expression
23 and evidence that their transcription is regulated by stem cell-specific transcription factors, we
24 hypothesized that CC-lincRNAs may contribute to the interplay between cell cycle and
25 maintenance of pluripotency in mESCs. If CC-lincRNAs participate in the network controlling
26 maintenance of mESC cell state, they should be co-expressed with genes involved in
27 maintenance of pluripotency. To test this hypothesis, we investigated the correlation, during
28 mESC neuronal commitment, between CC-genes and genes implicated in maintenance of
29 pluripotency [36]. First, we found that, consistent with the interplay between cell cycle control and
30 maintenance of mESC cell state, the median pairwise correlation between CC-PCGs and
31 pluripotency genes (Spearman's $r=0.06$) is similar to what is found for pairs of genes implicated
32 in pluripotency ($r=0.10$, two-tailed Wilcoxon test p -value=0.3, Figure 3G). Consistent with our
33 hypothesis that CC-lincRNAs contribute to maintenance of mESC cell state, we found that the

1 extent of their association with pluripotency genes ($r=0.05$) is also similar to what we estimate for
2 pairs of genes implicated in pluripotency (two-tailed Wilcoxon test p -value=0.7, Figure 3G). For
3 comparison, we also estimated the strength of the association with genes involved in pluripotency
4 for non-cell cycle differentially expressed mESC coding ($r=0.03$) and non-coding ($r=-0.01$) genes
5 and found this to be significantly lower than that of CC-lincRNAs or CC-mRNAs (two-tailed
6 Wilcoxon test p -value<0.05, Figure 3G). Similar results are obtained when considering only
7 significant correlations (correlation test p <0.05) between pluripotency gene and coding or
8 noncoding transcripts.

9 These results suggest that CC-lincRNAs modulate specific aspects of mESC cell cycle and may
10 contribute to the regulation of stem cell cycle adaptations.

11

12 **Candidate CC-lincRNA analysis supports lincRNA roles in cell cycle regulation**

13 Next, we aimed to experimentally validate the contributions of previously uncharacterized CC-
14 lincRNAs to mESC cell cycle regulation. Considering that relatively low transcript abundance may
15 limit individual lincRNA's ability to regulate cell cycle progression, we selected one modestly
16 expressed CC-lincRNA (XLOC_018328, hereafter lincCC1, Supplementary Figure 4A), and one
17 lincRNA that is relatively highly expressed (Gm26853, hereafter lincCC2, Supplementary Figure
18 4B) in mESCs (Figure 4A). We employed CRISPR activation (CRISPRa) to increase endogenous
19 lincRNAs' transcription. For each lincRNA, we designed 2 guide RNAs (gRNA) to target VP160
20 fused dead-Cas9 (dCas9-VP160) [37] to the vicinity of lincRNA promoters. As a control, we
21 designed a non-targeting scrambled gRNA. We transiently co-transfected each of the gRNA-
22 expressing constructs with a dCas9-VP160 expressing vector. Seventy-two hours post-
23 transfection we observed an average 2-fold upregulation (2-tailed unpaired t-test p -value < 0.05)
24 of candidate lincRNAs expression (Figure 4B-C) in mESCs treated with targeting gRNA, relative
25 to control.

26 To assess the impact of changes in candidate lincRNA expression upon cell cycle progression in
27 mESC, we determined the proportions of cells in G1, S and G2/M phases using Fluorescence
28 Activated Flow Cytometry (FACS). We used EdU incorporation and DNA content to identify the
29 proportion of single cells in each cell cycle phase following CC-lincRNA
30 overexpression(Supplementary Figure 4C). We found that, consistently with the proposed role of
31 lincCC1 and lincCC2 in the modulation of cell cycle progression, upregulation of these lincRNAs
32 is associated with significant changes in the proportion of cells within different cell cycle stages.
33 LincCC1 upregulation is associated with a significant increase in the number of cells in G2/M and

1 small, yet significant changes in the proportion of cells in G1 and S phases (Figure 4D). LincCC2
2 mostly affects the proportion of cells in G1. We have also investigated changes in cell cycle
3 markers, specifically *Ccnb1* and *Ccnd1*, whose expression in mESC is highest in G2/M and lowest
4 in G1. As expected, we found that lincCC1 upregulation is associated with a significant increase
5 in the two cell cycle markers (Figure 4E-F). Increased expression of lincCC2 moderately
6 decreased the expression of both markers which is consistent with the increase in the number of
7 cells in G1 (Figure 4G-H).

8 These observations are consistent with the role of these CC-lincRNAs in the regulation of cell
9 cycle progression.

10

11

1 CONCLUSION

2 The cell cycle is central to the development of a multicellular organism from a single cell zygote
3 and is required for cell renewal. Dysregulation of this process can cause disease, most notably
4 cancer. Progression through the cell cycle requires dynamic and tightly-regulated transitions
5 between well-defined cell-cycle stages, which are controlled by changes in cell cycle regulators'
6 activity. While control of cell cycle progression has been primarily assigned to protein-coding
7 genes, several lincRNAs have recently been shown to contribute to this process [8]. For example,
8 a recent siRNA screen in HeLa cells revealed that knockdown of 26 lincRNAs, whose expression
9 is deregulated in cancer, impacts different aspects of cell cycle progression [13]. The role of
10 lincRNAs in this process is further supported by a more recent comprehensive high-content RNAi
11 screen in the same cells [38]. In parallel, characterization of individual lincRNAs has also
12 illustrated how these noncoding RNAs contribute to the regulation of different aspects of cell cycle
13 [8].

14 In contrast to most cell cycle protein-coding regulators, lincRNA expression is often restricted in
15 time and space, as supported by the analysis of their expression across adult and embryonic
16 tissues and in single cells [for example [15, 16, 27]]. This suggests that most lincRNA-encoded
17 functions are tissue-specific. While lincRNAs have been previously implicated in the regulation of
18 cell cycle progression [10, 11, 23], their role, if any, in cell type-specific modulations of this central
19 biological process remains understudied. Here, we used mouse embryonic stem cell (mESC)
20 cycle, which is characterized by a truncated G1 phase, as a model system to assess the
21 contributions of lincRNAs expressed in mESCs to the modulation of this stem cell adaptation.

22 To identify lincRNAs that are putative cell cycle regulators, we reasoned that for noncoding genes
23 the functional moiety is the transcript, thus differential noncoding gene expression between cell
24 cycle stages would result in differential activity and enrich for lincRNAs with roles in cell cycle
25 regulation. Consistent with this hypothesis, our genome-wide analyses and experimental
26 validations support the role of lincRNAs differentially expressed between mESC cell cycle stages
27 as modulators of cell cycle progression, likely through interaction with other cell cycle regulators.

28 Interestingly and relative to protein-coding genes, whose activity during cell cycle is often
29 modulated by post-translational modifications, lincRNAs are enriched among differentially
30 expressed transcripts, supporting that in mESCs their expression is more frequently dynamic
31 throughout cell cycle progression. The fraction of cell cycle-regulated lincRNAs is similar to a
32 previous estimate done in HeLa cells using bulk RNA sequencing (~9%,[39]). However, the
33 dynamics of lincRNA expression throughout the cell cycle differs between cell types, as in contrast

1 with this earlier study in HeLa [39] that revealed no preferential cell stage specific expression in
2 mESCs, we found most lincRNA are highly expressed in G1 and differentially expressed between
3 G1 and S phase. Given the critical importance of the G1-S transition in maintenance of embryonic
4 stem cell state [32], we hypothesize that a subset of lincRNAs with roles in mESC cell cycle
5 progression also have roles in maintenance of stem cell state. Supporting this hypothesis is the
6 observation that these lincRNAs' expression is often restricted to pluripotent cells, and rapidly
7 decreases upon exit from pluripotency and entry into neural commitment. Furthermore the
8 expression of these lincRNAs is often regulated by core pluripotency transcription factors,
9 including Nanog, Sox2 and Oct4. Finally, we provide preliminary evidence that cell cycle lincRNAs
10 are part of the network underlying pluripotency.

11 While further work is now required to disentangle how individual lincRNAs may contribute to cell
12 cycle progression in mESCs, our results suggest that tissue-specific regulation by lincRNAs
13 contributes to cell-type specific adaptations of ubiquitous processes.

14

15

1

2 **METHODS**

3

4 **Processing of cell cycle staged single cell RNA sequencing data**

5 Mouse genome sequence and annotation files were downloaded from ENSEMBL (GRCm38.82
6 i.e. mm10). LincRNAs expressed in mESCs [17] were added to the transcript annotations using
7 custom Python scripts in order to appropriately deal with novel transcripts overlapping existing
8 loci, leading to a total of 55,596 loci. The FASTA sequences of the 96 ERCC spike-ins used in
9 the experiment were downloaded from UCSC GoldenPath. We used CGAT ([40], v 0.2.3) to
10 extract transcript sequences longer than 200 nucleotides, and Kallisto ([41], v 0.42.4, default
11 parameters) to build a transcriptome index that included 114,842 transcripts across 49,285 loci
12 and ERCCs. The FASTQ files for staged mESC single-cell RNA-sequencing were downloaded
13 from ArrayExpress (accession number E-MTAB-2805). For each cell, we estimated transcript
14 expression using Kallisto (v. 0.42.4) [41] without bootstraps. Hit counts were imported into R and
15 summarized to the gene level using tximport [42]. After removing genes without any hits in any
16 cells, only 38,016 genes remained.

17 Basic cell-level quality control was performed as previously described [20]. Briefly,
18 we excluded cells: 1) with a cell-wise gene detection rate below 20%; 2) cells with <1.6M total
19 hits; 3) cells with proportions of hits to ERCCs lower than 15% or higher than 65%; 4) cells with
20 a proportion of hits to mitochondrial genes lower than 1% or higher than 10%; and 5) cells with
21 an estimated cell size higher or lower than 2 median absolute deviations from the stage-median
22 cell size. In total, after these filtering steps, 94/95 G1 cells, 76/88 S cells, and 74/96 G2/M cells
23 were retained for further analysis.

24 We then performed gene-level quality control. We considered only genes that had at least one hit
25 count in at least 4% of samples. Hit counts were normalized using the scran package (v1.0.4,
26 [43]). Size factors were calculated using pools of samples of sizes 10 to 35 cells from each stage.
27 We used scLVM [20, 44] to filter out genes whose total variance is not significantly higher than
28 that expected from pure technical variability (fitTechnicalNoise parameters: mincv2=0.01,
29 quan=0.10 ; getVariableGenes parameters: threshold = 0.10, minBioDisp = 0.30), and
30 subsequently also removed ERCCs & mitochondrial genes. After this final filtering step, 10,487
31 genes were kept.

1 Except for differential expression analysis, where scran-normalised counts were used, all
2 subsequent analyses were performed on scran-normalised shifted log₁₀ counts ($sl_{10} =$
3 $\log_{10}(\text{normalised counts} + 1)$).

4

5 **Processing of bulk RNA sequencing for a time-course of mESC to neurons differentiation**

6 We used STAR [45] (v 2.5.3a) to map bulk RNA sequencing data for a 216-hour time course of
7 mESC differentiation into neurons [30] to the Mouse transcriptome. Transcript quantification was
8 performed using RSEM [46] (v 1.3.0) and for each time point we considered the average of
9 expression across time points. We estimated the Spearman correlation between genes of interest
10 and pluripotency associated genes [36] using R.

11

12 **Differential expression analysis**

13 Kallisto pseudo-count data was imported into R (v 3.3.1) and prepared for DESeq2 (v 1.12.4) [47]
14 using the *tximport* [42] package (v 1.0.3).

15 Principal Components Analysis (PCA) was applied using R package FactoMineR [48] to an
16 expression matrix consisting of all cells passing QC in rows, and all genes passing QC in columns.
17 The cell cycle signal typically appeared most strongly across the first two principal components,
18 with the third component correlating strongly with the gene dropout rate (not shown). Differentially
19 expressed genes (FDR < 5%, log₂ fold change > 0.1) were called between pairs of cell cycle
20 stages using DESeq2 [47, 49] using appropriate contrasts.

21 In order to assess whether the overall lower expression of lincRNAs affected our ability to call
22 them as DE, we performed a down-sampling experiment to bring mRNA expression down to
23 levels comparable to lincRNAs. We first estimated the average scaling factor between mRNA and
24 lincRNA expression in the original data. We estimated the difference between the median
25 Transcripts Per Million reads (TPM) in quality-controlled cells between lincRNAs and mRNAs to
26 be 14.196, i.e. on average mRNAs are 14x more highly expressed than lincRNAs. We randomly
27 sub-sampled the original FASTQ files to 1/14th of their original size (i.e. using a factor of 0.0714)
28 using *seqtk* (v 2015.10.15). We quantified transcript expression using Kallisto and filtered cells
29 and genes as described above prior to differential gene expression analysis. For the sub-sampled
30 data, the number of tested genes was similar to the full data (9 923 vs 10 391). We then counted
31 the number of mRNA genes called as DE in the full analysis that passed the quality control filters

1 for the sub-sampled data (388), and the number of those called as DE in the sub-sampled analysis
2 (233, i.e. 60.1%).

3

4 **Co-expression analysis.**

5 We considered a gene to be a cell cycle regulator if: 1) was annotated as a cell cycle gene [20];
6 2) it was annotated with a GO term containing the string “cell cycle” or 3) had a Human ortholog
7 annotated in CycleBase [21]. Pluripotency-associated genes were extracted from the ESCAPE
8 database [36].

9 Co-expression analysis with cell cycle genes was performed using the single cell RNA
10 sequencing data with staged mESCs [20]. We considered all loci expressed (normalized shifted
11 $\log_{10} > 0.14$) in at least 50 cells (out of a possible 244). The expression cut-off was defined based
12 on inspection of the shifted \log_{10} expression values. We estimated the Spearman correlation
13 between all these loci and considered a gene pair to be significantly correlated if the absolute
14 Spearman correlation between their expression was > 0.10 and the correlation test p-value was
15 < 0.10 . The correlation between any given pair was only calculated in cells where both genes
16 were expressed. Correlations for gene pairs where there were less than 20 such value pairs were
17 set to 0.

18 Co-expression analysis with pluripotency genes was performed using the time course of mESC
19 to neurons differentiation data, as described above.

20

21 **Enrichment analyses**

22 Enrichment analyses for Gene Ontology Biological Process, KEGG and REAC terms in *Mus*
23 *musculus* were carried out using R package “gProfileR” (v. 0.6.1) [50]. Terms were considered to
24 be significantly enriched if the associated corrected p-value was below 10% relative to the
25 specified background of mESC expressed genes.

26 Enrichment in binding of mESC transcription factors (TFs) [33] at CC-lincRNA promoters (defined
27 as +/-1 kb from their annotated TSS) was estimated using the Genome Association Tester (GAT)
28 [40]. GAT tests whether the enrichment of TF binding at CC-lincRNA promoters is different from
29 what would be expected based on 10,000 random samplings (with replacement) of intergenic
30 segments with the same length and GC content as the CC-lincRNA promoters. The gat-compare
31 tool was used to test the significance of the enrichment of TF binding at CC-lincRNA promoters
32 relative to that at non CC-lincRNA promoters. Core TF binding sites were obtained from [33].

1

2 **Loci tissue specificity metrics in Mouse**

3 We manually selected 150 Mouse paired-end total RNA bulk RNA-sequencing datasets from the
4 ENCODE project [51], covering a range of tissues, sexes and ages, and added 3 publicly-
5 available Mouse embryonic stem cell datasets [22]. We defined a “tissue.simple” grouping of
6 samples, based on a high-level description of the tissue of origin (e.g. central nervous system, or
7 heart) and of the developmental stage (adult or embryonic). Gene expression was estimated
8 using Kallisto and imported into R using tximport as described above. Library size normalization
9 was performed with DESeq2, and counts were transformed into shifted log₁₀ normalised values.
10 Values below a background level of 0.1 were set to 0. This cut-off was obtained based on the
11 distribution of shifted log₁₀ expression values. Genes with no expression values above 0 in any
12 sample were discarded. Expression values were averaged across technical and biological
13 replicates using the median. Tau was calculated as described in [29], briefly as $\text{Tau} = \sum(1 -$
14 $(v/\max(v)))/(\text{length}(v)-1)$, where v is a vector of average expression values for different tissues.

15

16 **Cell Culture**

17 ES-E14-Tg2a (E14) cells were grown on 0.1% gelatin-coated tissue culture dishes, in DMEM
18 (Thermo Fischer, 41965-039) supplemented with 1x Non-Essential Amino Acids (Thermo Fischer
19 11140-035), 50 μM β -mercaptoethanol (Thermo Fischer 31350-10), 15% Fetal Bovine Serum
20 (Thermo Fischer 10499-044), 500 Units/ml of Penicillin/Streptomycin (Thermo Fischer,
21 15140122), and 100 Units/ml of Recombinant mouse LIF Protein (Merck ESG1107). Culture were
22 seeded at an average density of $\sim 3.8 \times 10^4$ cells/cm² and passaged every 48 h.

23

24 **Analysis of cell cycle stage gene expression**

25 We resuspended 10^6 cells in 1 ml of PBS, containing 1 $\mu\text{L}/\text{mL}$ of fluorescent reactive dye
26 (LIVE/DEAD) and incubated in the dark for 30 minutes at room temperature. Cells were then
27 washed with PBS, spun, and resuspended in fresh medium. We add 2 μL of DNA Hoechst 33324
28 dye (20 mM) and cells were incubated at 37°C for 20 minutes. Following incubation, cells were
29 centrifuged at 4°C for 4 minutes at 400 g and the resulting cell pellet was resuspended in 500 μl
30 of 3% FBS in PBS with 0.1% EDTA and kept on ice. Unstained and single dye controls prepared
31 in parallel were used for FACS calibration.

1 Cells were sorted in an AstriosEQ (Beckmann Coulter) cell sorter and collected in 500 uL of RTL
2 buffer from the RNAeasy extraction kit (QIAGEN). Forward and side scatter (FSC & SSC, 488nm
3 DPSS laser) were used as is common for size and doublet exclusion. We excluded dead cells
4 based on LIVE/DEAD fluorescence (488nm DPSS laser) and used DNA content (355nm DPSS
5 laser) to define three gates: G1, S and G2/M (Supplementary Figure 5).
6 RNA was extracted using RNeasy mini kit (Qiagen) according to manufacturer's instructions. RNA
7 was reverse transcribed using Quatitect Reverse Transcription Kit (Qiagen 205313). Quantitative
8 PCR analysis was performed using SYBR Green Quantitative PCR Master Mix (Roche
9 0692404001) in a Light Cycler 96 Real Time PCR system (Roche). Briefly, the RTqPCR reaction
10 was assembled in 10uL with forward and reverse primers at a final concentration of .5 uM each,
11 and SYBR Green Quantitative PCR Master Mix at a final concentration of 1X.

12

13 **Candidate lincRNA overexpression and cell cycle analysis.**

14 We used E-CRISPR [52] to design 2 guide RNA (gRNA) sequences located within 1 kb of lincCC1
15 and lincCC2 promoters respectively. We synthesized oligos containing these sequences and BbsI
16 restriction sites. Annealed oligos were inserted into the pKLV-U6gRNA(BbsI)-PGKpuro2ABFP
17 vector [53].

18 We seeded 1.5×10^5 E14 cells/well in 6-well plates and allowed cells to grow overnight. We used
19 lipofectamine 2000 (Thermo Fischer) to transfect 1000 ng of gRNA expression vector and 1000
20 ng of pAC95-pmax-dCas9-Vp160-2A-Neo [37] vector into mESC cultures overnight according to
21 manufacturer's instructions. We replaced growth medium 8 hours after transfection to minimize
22 toxicity. Seventy-two hours post transfection one sample was collected for RNA to ensure the
23 efficiency of the over-expression by qPCR; in parallel the other cells were pulsed with 10 uM Edu
24 for 30 minutes in the dark at 37°C. Cells were washed with 1% BSA in PBS and trypsinized cells.
25 Following a second wash with 1% BSA in PBS, cells were fixed at room temperature, protected
26 from the light for 15 minutes in 100 uL of Click-iT fixative solution. After fixation, cells were washed
27 in 1% BSA in PBS, resuspended in 100 uL of 1x Click-iT saponin-based permeabilization and
28 wash reagent, and incubated at room temperature in the dark for 15 minutes. Following
29 incubation, 500 uL of Click-iT reaction cocktail containing Alexa Fluor 488 Fluorescent Dye Azide
30 were added and samples were incubated at room temperature in the dark for 30 minutes.
31 Reaction was quenched by resuspending cells in 1 mL of 1x Click-iT saponin-based
32 permeabilization reagent. To stain the samples for DNA content, 1 uL of Fx Cycle FarRed staining
33 solution (Thermo Fischer F10348) was added to each sample, and Pure Link RNase A (Thermo

1 Fischer 12091039) was added at a final concentration of 100 ng/mL. The samples were incubated
2 at 4°C in the dark for 30 minutes, analyzed by flow cytometry analysis. Cells stained for DNA
3 incorporation and content were analyzed using a 10 color/3 laser Beckman Coulter Gallios
4 Analyzer. Blue (405 nm) and red (640 nm) excitation lasers were used for excitation of the Alexa
5 Fluor 488 Fluorescent Dye Azide and Fx FarCycle Red respectively. Emission was detected using
6 channels FL-09 and FL-06 for Alexa Fluor 488 and Fx FarCycle Red respectively. Three
7 independent experiments were carried out for both candidate lincRNAs with at least 3 biological
8 replicates each. 30-60k events were flowed per sample, except for the first experiment where 15-
9 30k events were flowed.

10 Flow data was analyzed in FlowJo (v10.2). Flow events were gated on Cells and Singlets, and
11 spillover was compensated. Low incorporation 2n and 4n populations, as well as a medium-to-
12 high incorporation population, were easily identifiable in the DNA incorporation vs content
13 scatterplot, and gated respectively as G1, G2/M and S (and ungated). This stage-level gating was
14 performed by two gaters, blind to the direction and amplitude of target lincRNA expression
15 modulation. Stage population fractions were comparable between gaters (Pearson correlations
16 between stage fractions 0.65-0.97 depending on stage & experiment), and thus all results
17 presented here are those of one gater.

18 Sample-level summaries of the flow cytometry results were generated using FlowJo (v10.2).
19 Summaries were imported into R. Samples were quality-controlled based on their percentages of
20 cells/singlets (indicative of cell health), and MFIs (indicative of staining strength). Experiments for
21 which the associated qPCRs did not validate over-expression of the targets were excluded.
22 Ultimately, 26 samples from 2 experiments and 5 treatment groups (scrambled, two different
23 guides for lincCC1 and two for lincCC2) were retained. Differences in the percentages of cells in
24 each stage were assessed between mock and treatment conditions using unpaired unequal
25 variance t-tests.

26

27 **Acknowledgments**

28 pKLV-U6gRNA-EF(BbsI)-PGKpuro2ABFP was a gift from Hiroshi Ochiai (Addgene plasmid #
29 62348 ; <http://n2t.net/addgene:62348> ; RRID:Addgene_62348), pAC95-pmax-dCas9VP160-2A-
30 neo was a gift from Rudolf Jaenisch (Addgene plasmid # 48227 ; <http://n2t.net/addgene:48227> ;
31 RRID:Addgene_48227).

32 We would like to thank the University of Lausanne Flow Cytometry Platform with help with FACS
33 and sorting analysis. The computations were performed at the Vital-IT (<https://www.vital-it.ch>)

1 Center for high-performance computing of the SIB Swiss Institute of Bioinformatics. We would
2 like to thank Dario Bottinelli for technical support during the early stages of this project and Vincent
3 Dion and Constance Ciaudo for reading and commenting on early versions of this manuscript.
4 This work was funded by the Swiss National Science Foundation (grant PP00P3_150667 to
5 A.C.M) and the NCCR in RNA & Disease (A.C.M.).

6

7 **Authors Contributions**

8 AATS, AB and ACM contributed to the study design. AATS and JYT performed the insilico
9 analysis. AATS, AB, MFS, BA and ACM performed the *in vitro* analysis. ACM supervised the
10 study. ACM and AATS wrote the manuscript. All coauthors read and approved the manuscript.

11

12

13

14

15

1 **Figure legends**

2 **Figure 1: lincRNA expression is often cell cycle regulated**

3 **A)** Principal component analysis of gene expression for all loci passing the technical noise filter.
4 The first 2 principal components (PC1 on the x-axis and PC2 on the y-axis) together explain 5.15
5 % of the total variability, and separate cells in different cell cycle stages (G1: orange, S: blue;
6 G2/M: green). **B)** Percentage of protein-coding genes (left) and lincRNAs (right) that are
7 differentially expressed (dark grey, numbers indicate the percentage) between at least 2 cell cycle
8 stages. **C)** Fold difference in normalized expression (relative to G1) of known cell cycle regulated
9 genes (Ccnb1, Ccnd1, Ccne1, Neat1) and 2 differentially expressed novel lincRNAs (lincCC1 and
10 lincCC2) in mESCs at different cell cycle stages (G1: orange, S: blue, G2/M: green). Significance
11 (two-tailed unpaired t-test p-value) between cell cycle stage expression is indicated as: NS p>
12 0.05, * p<0.05, ** p<0.01, *** p<0.001.

13

14

15 **Figure 2: Genes differentially expressed between cell cycle stages have cell cycle related** 16 **functions.**

17 **A)** Results of the GO term enrichment analysis for cell cycle stage differentially expressed genes.
18 Grey bars indicate the fold enrichment, and points the associated $-\log_{10}$ of the p-value. Dashed
19 line indicates the 10% FDR cutoff. Distribution of the percentage of genes cell cycle regulators
20 that are significantly correlated in expression with **B)** protein-coding genes and **C)** lincRNAs.
21 Differentially or non-differentially expressed genes from each biotope are represented in dark and
22 light grey respectively. Significance of the distribution comparison (two-tailed Mann-Whitney-
23 Wilcoxon rank-sum test) are indicated as: *** p-value < 0.001.

24

25

26 **Figure 3: CC-lincRNAs are associated with stem cell cycle adaptations**

27 **A)** Distribution of tissue specificity (measured as Tau) for CC-lincRNAs, CC-PCGs, and annotated
28 cell cycle genes. Distribution of the fold difference in expression of **B)** lincRNAs and **C)** protein-
29 coding genes during a 216-hour neuronal commitment of mESCs. Fold difference in expression
30 is relative to the median fold difference at time=8 hours. **D)** Fold enrichment in binding (bars, x
31 axis) of pluripotency transcription factors (y-axis) for CC-PCGs (dark grey) and CC-mRNAs (light

1 grey). **E**) Cell cycle stage-average (G1: orange, S: blue, G2/M: green) of the expression Z-scores
2 of CC-PCGs (left panel) and CC-lincRNAs (right panel). **F**) Percentage of protein-coding genes
3 (left) and lincRNAs (right) differentially expressed between G1 vs S (orange), G1 vs G2M (blue)
4 or S vs G2/M (green). **G**) Distribution of the correlations between pairs of pluripotency-associated
5 genes (black) or known pluripotency genes, and differentially expressed (CC, grey) or non-
6 differentially expressed (nonCC, white) protein-coding genes and lincRNAs. Significance (two-
7 tailed Mann-Whitney-Wilcoxon rank-sum test) for the comparison between pluripotency-
8 associated genes and the different gene classes is indicated on top of the boxplot as: NS $p > 0.05$,
9 ** $p < 0.01$, *** $p < 0.001$.

10

11 **Figure 4: Candidate lincRNA overexpression impacts cell cycle progression**

12 **A**) Histogram of the mean cell expression of all considered loci in mESCs. Lines indicate the
13 expression of lincCC1 and lincCC2. Relative **B**) lincCC1 and **C**) lincCC2 expression 72 h after
14 co-transfection of Cas9-VP160 with scramble-, gRNA1- or gRNA2-expressing constructs. **D**)
15 Percentage of mESCs at G1, S and G2/M stages of the cell cycle 72 h post-transfection of mESCs
16 with scramble (white), lincCC1 (dark grey) or lincCC2 (light grey) targeting gRNAs. Relative
17 expression of *Ccnb1* (**E-G**) and *Ccnd1* (**F-H**) 72 h post-transfection of mESCs with scramble
18 (white), lincCC1 (dark grey) or lincCC2 (light grey) targeting gRNAs. Significance (two-tailed
19 unpaired t-test p-value) of comparisons is indicated as: NS $p > 0.05$, * $p < 0.05$, ** $p < 0.01$, ***
20 $p < 0.001$.

21

22 **Supplementary Figure 1:**

23 **A**) Schematic representation of the differential expression analysis pipeline. **B**) Scatterplot
24 showing for each sample (cell) the total hit (mapped read) counts & “Cell Detection Rate”, i.e.
25 fraction of genes detected by at least 1 hit in each cell. Low library quality exclusion thresholds
26 are indicated by dashed magenta lines. Cells are coloured by cell cycle stage. **C**) Scatterplot
27 showing for each cell the percent hits to mitochondrial (MT) genes & to ERCC spike-ins. Low
28 library quality thresholds are indicated by dashed magenta lines. **D**) Distributions of Buettner’s
29 cell size ratio [20] for cells in each stage. Magenta lines show medians +/- 2 median absolute
30 deviations; cells falling outside of these windows are excluded. **E**) Technical noise filter [44] as
31 implemented in scLVM [20]: each gene is represented by its cross-sample mean expression (x-
32 axis) and coefficient of variation (squared: CV², y-axis). Blue dots correspond to ERCC spike-ins,
33 while the green line represents the non-linear CV² ~ mean model that was fit to the spike-ins, and

1 then used to test which genes show significantly higher-than-technical variability. Genes in black
2 do not pass the significance test, those in red do. Counts of genes passing the test are indicated
3 in the top-right hand corner.

4

5 **Supplementary Figure 2:**

6 **A)** boxplots of cross-sample mean expression (normalised shifted log10 counts) for genes of
7 various classes: all=tested for differential expression. DE=differentially-expressed. NDE: non-
8 differentially expressed. mRNA: protein-coding genes. lincRNA: lincRNA loci. **B)** Boxplots of
9 shifted log10 mean loci expression for protein-coding genes (mRNA, dark grey) and lincRNAs
10 (light grey), in both the sub-sampled (1/14th) data (SS) and FULL data from cell cycle staged
11 single-cell RNAseq dataset [20].

12

13 **Supplementary Figure 3:**

14 Fold difference in relative expression for 9 predicted cell-cycle differentially expressed lincRNAs.

15

16 **Supplementary Figure 4:**

17 Genome browser view of the genomic location (mm10) of **A)** lincCC1 and **B)** lincCC2. Blue bars
18 indicate conservation in multiZ alignments (60 vertebrates). **C)** gating strategy to identify cells
19 from distinct cell cycle stages. Panel 1 shows the size exclusion gate based on FSC-H & SSC-H
20 for removing debris. Panels 2 shows the FSC-H vs FSC-A doublet exclusion gate; a similar gate
21 was implemented for SSC-H vs SSC-A. Panel 3 shows the partitioning of cells into 3 stages based
22 on DNA content (measured on FL6-A) and EdU incorporation (measured on FL1-A).

23

24 **Supplementary Figure 5:**

25 Histogram of cellular DNA content measures as stained by DAPI, showing gates for delineating
26 clearly-defined G1, S or G2/M stages.

27

28

1 References

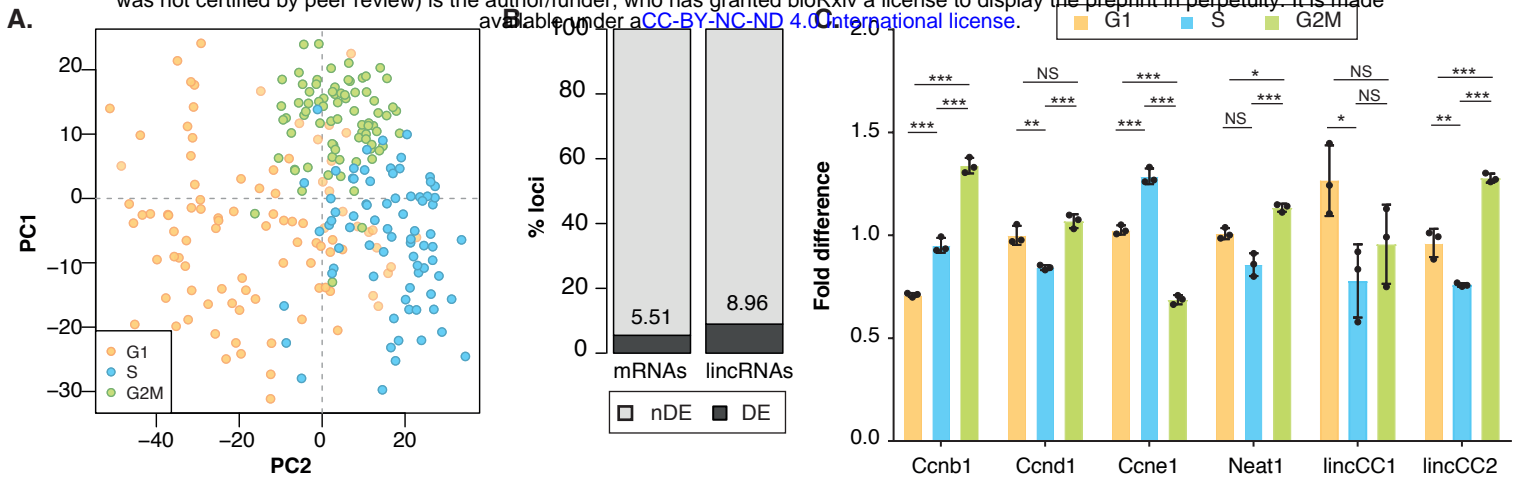
2

- 3 1. Murray A, Hunt T: *The Cell Cycle, an introduction*. Oxford University Press; 1993.
- 4 2. Morgan DO: **Principles of CDK regulation**. *Nature* 1995, **374**:131-134.
- 5 3. Weinberg RA: **The retinoblastoma protein and cell cycle control**. *Cell* 1995, **81**:323-
6 330.
- 7 4. Zaveri L, Dhawan J: **Cycling to Meet Fate: Connecting Pluripotency to the Cell Cycle**.
8 *Front Cell Dev Biol* 2018, **6**:57.
- 9 5. Soufi A, Dalton S: **Cycling through developmental decisions: how cell cycle dynamics
10 control pluripotency, differentiation and reprogramming**. *Development* 2016,
11 **143**:4301-4311.
- 12 6. Lee J, Go Y, Kang I, Han YM, Kim J: **Oct-4 controls cell-cycle progression of
13 embryonic stem cells**. *Biochem J* 2010, **426**:171-181.
- 14 7. Zhang X, Neganova I, Przyborski S, Yang C, Cooke M, Atkinson SP, Anyfantis G, Fenyk
15 S, Keith WN, Hoare SF, et al: **A role for NANOG in G1 to S transition in human
16 embryonic stem cells through direct binding of CDK6 and CDC25A**. *J Cell Biol* 2009,
17 **184**:67-82.
- 18 8. Kitagawa M, Kitagawa K, Kotake Y, Niida H, Ohhata T: **Cell cycle regulation by long
19 non-coding RNAs**. *Cell Mol Life Sci* 2013, **70**:4785-4794.
- 20 9. Sun Y, Ma L: **New Insights into Long Non-Coding RNA MALAT1 in Cancer and
21 Metastasis**. *Cancers (Basel)* 2019, **11**.
- 22 10. Tripathi V, Shen Z, Chakraborty A, Giri S, Freier SM, Wu X, Zhang Y, Gorospe M, Prasanth
23 SG, Lal A, Prasanth KV: **Long noncoding RNA MALAT1 controls cell cycle
24 progression by regulating the expression of oncogenic transcription factor B-MYB**.
25 *PLoS Genet* 2013, **9**:e1003368.
- 26 11. Marchese FP, Grossi E, Marin-Bejar O, Bharti SK, Raimondi I, Gonzalez J, Martinez-
27 Herrera DJ, Athie A, Amadoz A, Brosh RM, Jr., Huarte M: **A Long Noncoding RNA
28 Regulates Sister Chromatid Cohesion**. *Mol Cell* 2016, **63**:397-407.
- 29 12. Schmitt AM, Chang HY: **Long Noncoding RNAs in Cancer Pathways**. *Cancer Cell* 2016,
30 **29**:452-463.
- 31 13. Notzold L, Frank L, Gandhi M, Polycarpou-Schwarz M, Gross M, Gunkel M, Beil N, Erfle
32 H, Harder N, Rohr K, et al: **The long non-coding RNA LINC00152 is essential for cell
33 cycle progression through mitosis in HeLa cells**. *Sci Rep* 2017, **7**:2265.
- 34 14. Yan P, Luo S, Lu JY, Shen X: **Cis- and trans-acting lncRNAs in pluripotency and
35 reprogramming**. *Curr Opin Genet Dev* 2017, **46**:170-178.
- 36 15. Derrien T, Johnson R, Bussotti G, Tanzer A, Djebali S, Tilgner H, Guernec G, Martin D,
37 Merkel A, Knowles DG, et al: **The GENCODE v7 catalog of human long noncoding
38 RNAs: analysis of their gene structure, evolution, and expression**. *Genome Res*
39 2012, **22**:1775-1789.
- 40 16. Tuck AC, Natarajan KN, Rice GM, Borawski J, Mohn F, Rankova A, Flemr M, Wenger A,
41 Nutiu R, Teichmann S, Buhler M: **Distinctive features of lincRNA gene expression
42 suggest widespread RNA-independent functions**. *Life Sci Alliance* 2018,
43 **1**:e201800124.

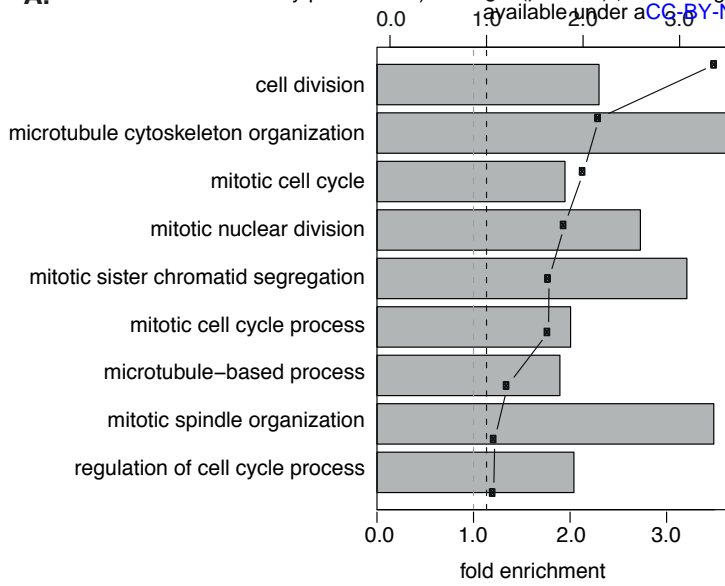
- 1 17. Tan JY, Vance KW, Varela MA, Sirey T, Watson LM, Curtis HJ, Marinello M, Alves S,
2 Steinkraus B, Cooper S, et al: **Cross-talking noncoding RNAs contribute to cell-**
3 **specific neurodegeneration in SCA7.** *Nat Struct Mol Biol* 2014, **21**:955-961.
- 4 18. Clark MB, Johnston RL, Inostroza-Ponta M, Fox AH, Fortini E, Moscato P, Dinger ME,
5 Mattick JS: **Genome-wide analysis of long noncoding RNA stability.** *Genome Res*
6 2012, **22**:885-898.
- 7 19. Mukherjee N, Calviello L, Hirsekorn A, de Pretis S, Pelizzola M, Ohler U: **Integrative**
8 **classification of human coding and noncoding genes through RNA metabolism**
9 **profiles.** *Nat Struct Mol Biol* 2017, **24**:86-96.
- 10 20. Buettner F, Natarajan KN, Casale FP, Proserpio V, Scialdone A, Theis FJ, Teichmann SA,
11 Marioni JC, Stegle O: **Computational analysis of cell-to-cell heterogeneity in single-**
12 **cell RNA-sequencing data reveals hidden subpopulations of cells.** *Nat Biotechnol*
13 2015, **33**:155-160.
- 14 21. Santos A, Wernersson R, Jensen LJ: **Cyclebase 3.0: a multi-organism database on**
15 **cell-cycle regulation and phenotypes.** *Nucleic Acids Res* 2015, **43**:D1140-1144.
- 16 22. Tan JY, Sirey T, Honti F, Graham B, Piovesan A, Merckenschlager M, Webber C, Ponting
17 CP, Marques AC: **Extensive microRNA-mediated crosstalk between lncRNAs and**
18 **mRNAs in mouse embryonic stem cells.** *Genome Res* 2015, **25**:655-666.
- 19 23. Adriaens C, Standaert L, Barra J, Latil M, Verfaillie A, Kalev P, Boeckx B, Wijnhoven PW,
20 Radaelli E, Vermi W, et al: **p53 induces formation of NEAT1 lncRNA-containing**
21 **paraspeckles that modulate replication stress response and chemosensitivity.** *Nat*
22 *Med* 2016, **22**:861-868.
- 23 24. Yu X, Li Z, Zheng H, Chan MT, Wu WK: **NEAT1: A novel cancer-related long non-**
24 **coding RNA.** *Cell Prolif* 2017, **50**.
- 25 25. Patterson DG, Roberts JT, King VM, Houserova D, Barnhill EC, Crucello A, Polska CJ,
26 Brantley LW, Kaufman GC, Nguyen M, et al: **Human snoRNA-93 is processed into a**
27 **microRNA-like RNA that promotes breast cancer cell invasion.** *NPJ Breast Cancer*
28 2017, **3**:25.
- 29 26. Lal A, Navarro F, Maher CA, Maliszewski LE, Yan N, O'Day E, Chowdhury D, Dykxhoorn
30 DM, Tsai P, Hofmann O, et al: **miR-24 Inhibits cell proliferation by targeting E2F2,**
31 **MYC, and other cell-cycle genes via binding to "seedless" 3'UTR microRNA**
32 **recognition elements.** *Mol Cell* 2009, **35**:610-625.
- 33 27. Ulitsky I, Bartel DP: **lincRNAs: genomics, evolution, and mechanisms.** *Cell* 2013,
34 **154**:26-46.
- 35 28. Yue F, Cheng Y, Breschi A, Vierstra J, Wu W, Ryba T, Sandstrom R, Ma Z, Davis C, Pope
36 BD, et al: **A comparative encyclopedia of DNA elements in the mouse genome.** *Nature*
37 2014, **515**:355-364.
- 38 29. Kryuchkova-Mostacci N, Robinson-Rechavi M: **A benchmark of gene expression**
39 **tissue-specificity metrics.** *Brief Bioinform* 2017, **18**:205-214.
- 40 30. Sun N, Yu X, Li F, Liu D, Suo S, Chen W, Chen S, Song L, Green CD, McDermott J, et al:
41 **Inference of differentiation time for single cell transcriptomes using cell population**
42 **reference data.** *Nat Commun* 2017, **8**:1856.
- 43 31. Chambers I, Tomlinson SR: **The transcriptional foundation of pluripotency.**
44 *Development* 2009, **136**:2311-2322.

- 1 32. Boward B, Wu T, Dalton S: **Concise Review: Control of Cell Fate Through Cell Cycle**
2 **and Pluripotency Networks.** *Stem Cells* 2016, **34**:1427-1436.
- 3 33. Chen X, Xu H, Yuan P, Fang F, Huss M, Vega VB, Wong E, Orlov YL, Zhang W, Jiang J,
4 et al: **Integration of external signaling pathways with the core transcriptional network**
5 **in embryonic stem cells.** *Cell* 2008, **133**:1106-1117.
- 6 34. Cho RJ, Huang M, Campbell MJ, Dong H, Steinmetz L, Sapinoso L, Hampton G, Elledge
7 SJ, Davis RW, Lockhart DJ: **Transcriptional regulation and function during the human**
8 **cell cycle.** *Nat Genet* 2001, **27**:48-54.
- 9 35. Whitfield ML, Sherlock G, Saldanha AJ, Murray JI, Ball CA, Alexander KE, Matese JC,
10 Perou CM, Hurt MM, Brown PO, Botstein D: **Identification of genes periodically**
11 **expressed in the human cell cycle and their expression in tumors.** *Mol Biol Cell* 2002,
12 **13**:1977-2000.
- 13 36. Xu H, Baroukh C, Dannenfelser R, Chen EY, Tan CM, Kou Y, Kim YE, Lemischka IR,
14 Ma'ayan A: **ESCAPE: database for integrating high-content published data collected**
15 **from human and mouse embryonic stem cells.** *Database (Oxford)* 2013, **2013**:bat045.
- 16 37. Cheng AW, Wang H, Yang H, Shi L, Katz Y, Theunissen TW, Rangarajan S, Shivalila CS,
17 Dadon DB, Jaenisch R: **Multiplexed activation of endogenous genes by CRISPR-on,**
18 **an RNA-guided transcriptional activator system.** *Cell Res* 2013, **23**:1163-1171.
- 19 38. Lovorka Stojic ATLL, Patrice Mascalchi, Christina Ernst, Aisling M, Redmond JM, Alexis R
20 Barr, Vicky Bousgouni, Chris Bakal, John C Marioni, Duncan T Odom, Fanni Gergely: **A**
21 **high-content RNAi screen reveals multiple roles for long noncoding RNAs in cell**
22 **division.** 2019.
- 23 39. Dominguez D, Tsai YH, Gomez N, Jha DK, Davis I, Wang Z: **A high-resolution**
24 **transcriptome map of cell cycle reveals novel connections between periodic genes**
25 **and cancer.** *Cell Res* 2016, **26**:946-962.
- 26 40. Heger A, Webber C, Goodson M, Ponting CP, Lunter G: **GAT: a simulation framework**
27 **for testing the association of genomic intervals.** *Bioinformatics* 2013, **29**:2046-2048.
- 28 41. Bray NL, Pimentel H, Melsted P, Pachter L: **Near-optimal probabilistic RNA-seq**
29 **quantification.** *Nat Biotechnol* 2016, **34**:525-527.
- 30 42. Soneson C, Love MI, Robinson MD: **Differential analyses for RNA-seq: transcript-level**
31 **estimates improve gene-level inferences.** *F1000Res* 2015, **4**:1521.
- 32 43. Lun AT, McCarthy DJ, Marioni JC: **A step-by-step workflow for low-level analysis of**
33 **single-cell RNA-seq data with Bioconductor.** *F1000Res* 2016, **5**:2122.
- 34 44. Brennecke P, Anders S, Kim JK, Kolodziejczyk AA, Zhang X, Proserpio V, Baying B, Benes
35 V, Teichmann SA, Marioni JC, Heisler MG: **Accounting for technical noise in single-**
36 **cell RNA-seq experiments.** *Nat Methods* 2013, **10**:1093-1095.
- 37 45. Dobin A, Davis CA, Schlesinger F, Drenkow J, Zaleski C, Jha S, Batut P, Chaisson M,
38 Gingeras TR: **STAR: ultrafast universal RNA-seq aligner.** *Bioinformatics* 2013, **29**:15-
39 21.
- 40 46. Li B, Dewey CN: **RSEM: accurate transcript quantification from RNA-Seq data with**
41 **or without a reference genome.** *BMC Bioinformatics* 2011, **12**:323.
- 42 47. Love MI, Huber W, Anders S: **Moderated estimation of fold change and dispersion for**
43 **RNA-seq data with DESeq2.** *Genome Biol* 2014, **15**:550.

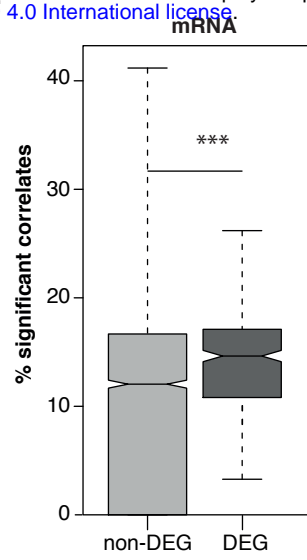
- 1 48. Le S, Josse J, Husson F: **FactoMineR: An R package for multivariate analysis**. *Journal*
2 *of Statistical Software* 2008, **25**:1-18.
- 3 49. Jaakkola MK, Seyednasrollah F, Mehmood A, Elo LL: **Comparison of methods to detect**
4 **differentially expressed genes between single-cell populations**. *Brief Bioinform* 2017,
5 **18**:735-743.
- 6 50. Reimand J, Arak T, Adler P, Kolberg L, Reisberg S, Peterson H, Vilo J: **g:Profiler-a web**
7 **server for functional interpretation of gene lists (2016 update)**. *Nucleic Acids Res*
8 2016, **44**:W83-89.
- 9 51. Consortium EP: **An integrated encyclopedia of DNA elements in the human genome**.
10 *Nature* 2012, **489**:57-74.
- 11 52. Heigwer F, Kerr G, Boutros M: **E-CRISP: fast CRISPR target site identification**. *Nat*
12 *Methods* 2014, **11**:122-123.
- 13 53. Ochiai H, Sugawara T, Yamamoto T: **Simultaneous live imaging of the transcription**
14 **and nuclear position of specific genes**. *Nucleic Acids Res* 2015, **43**:e127.
- 15



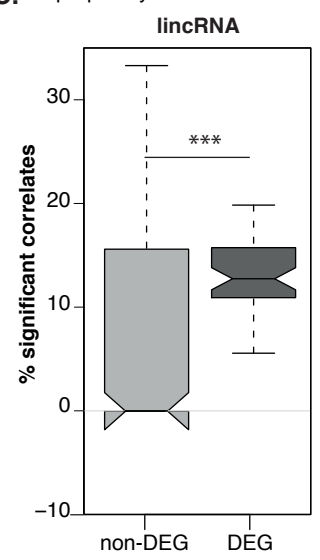
A.



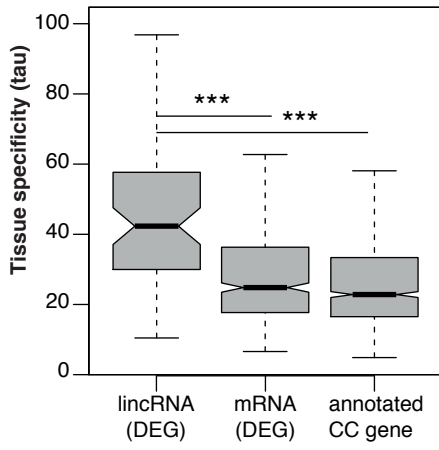
B.



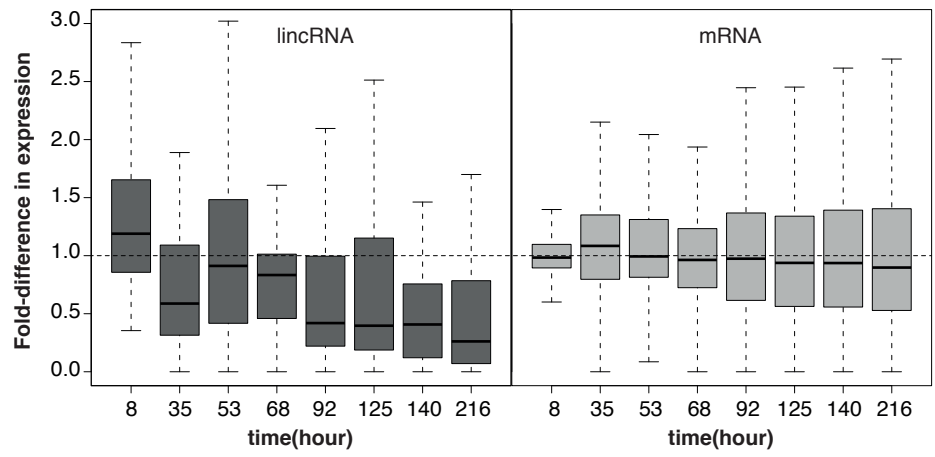
C.



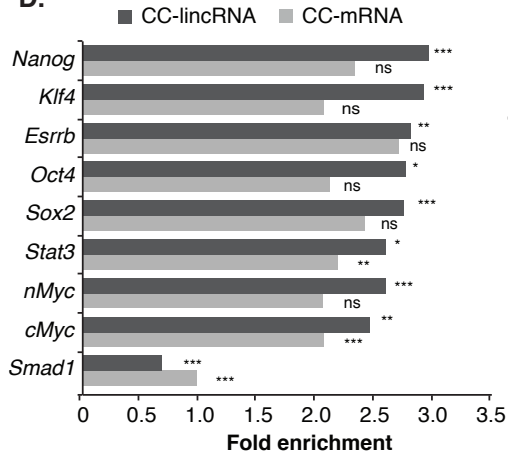
A.



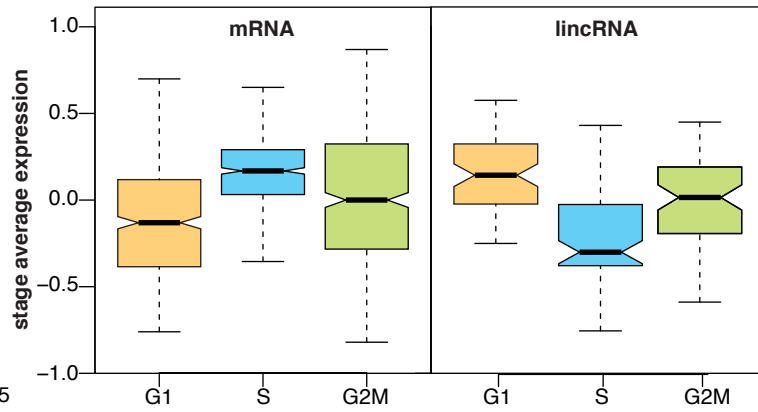
B.



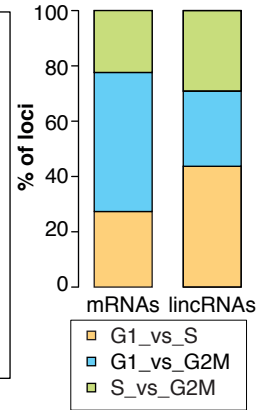
D.



E.



F.



G.

